Geomorphology 253 (2016) 217–224

Contents lists available at ScienceDirect

Geomorphology

journal homepage: www.elsevier.com/locate/geomorph

Soil erosion rates in two karst peak-cluster depression basins of northwest Guangxi, China: Comparison of the RUSLE model with ^{137}Cs measurements

Teng Feng [a,b,c], Hongsong Chen [a,b,*], Viktor O. Polyakov [d], Kelin Wang [a,b], Xinbao Zhang [e], Wei Zhang [a,b]

[a] Key Laboratory of Agro-ecological Processes in Subtropical Region, Institute of Subtropical Agriculture, Chinese Academy of Sciences, Changsha, Hunan 410125, China
[b] Huanjiang Observation and Research Station for Karst Ecosystems, Chinese Academy of Sciences, Huanjiang, Guangxi 547100, China
[c] University of Chinese Academy of Sciences, Beijing 100049, China
[d] Southwest Watershed Research Center, USDA-ARS, Tucson 85719, USA
[e] Key Laboratory of Mountain Environment Evolvement and Regulation, Institute of Mountain Hazards and Environment, Chinese Academy of Sciences, Sichuan 610041, China

ARTICLE INFO

Article history:
Received 4 April 2015
Received in revised form 18 October 2015
Accepted 20 October 2015
Available online 21 October 2015

Keywords:
Karst
RUSLE
Calibration
Slope length
^{137}Cs

ABSTRACT

Reliable estimation of erosion in karst areas is difficult because of the heterogeneous nature of infiltration and subsurface drainage. Understanding the processes involved is a key requirement for managing against karst rock desertification. This study used the revised Universal Soil Loss Equation (RUSLE) to estimate the annual soil erosion rates on hillslopes and compared them with ^{137}Cs budget in the depressions at two typical karst peak-cluster depression basins in northwest Guangxi, southwestern China. Runoff plots data were used to calibrate the slope length factor (L) of the RUSLE model by adjusting the accumulated area threshold. The RUSLE model was sensitive to the value of the threshold and required DEMs with 1 m resolution, due to the discontinuous nature of the overland flow. The average annual soil erosion rates on hillslopes simulated by the RUSLE were 0.22 and 0.10 Mg ha^{-1} y^{-1} during 2006 through 2011 in the partially cultivated GZ1 and the undisturbed GZ2 basins, respectively. The corresponding deposition rates in the depressions agreed well with the ^{137}Cs records when recent changes in precipitation and land use were taken into consideration. The study suggests that attention should be given to the RUSLE-L factor when applying the RUSLE on karst hillslopes because of the discontinuous nature of runoff and significant underground seepage during storm events that effectively reduces the effects of slope length.

1. Introduction

Karst landscapes are areas in which corrosion and dissolution of carbonate bedrock are dominant geomorphic processes. They occupy approximately 12% of continental terrains and have highly fragile environments (Febles-Gonzalez et al., 2012). Soil erosion and progressive degradation have been identified as severe geo-environmental hazards in many karst areas (Parise et al., 2009). In southwestern China, karst areas cover nearly 42.6×10^4 km^2 with a population of about 100 million. Heavy population pressure has accelerated the rock desertification and land degradation of karst environments (Wang et al., 2004). A thorough understanding of the distributions of soil loss and sediment yield is an urgent and basic requirement for local land managers to assess landscape changes and develop soil conservation policies for karst areas.

The Universal Soil Loss Equation (USLE) model is a widely used empirical soil erosion model for computing annual unit-plot erosion in various field conditions. The model generates estimated erosion by multiplying the factors of rainfall erosivity (R), soil erodibility (K), slope length and steepness (LS), cover management (C) and support practice (P) (Wischmeier and Smith, 1978). RUSLE is the revised version of USLE, which has been used at various spatial scales by subdividing an area of applications into subareas with homogeneous factors and combined with GIS methodology (Renard et al., 1991). This model has been used in karst terrains of Cuba and southwestern China (Xu et al., 2009; Febles-Gonzalez et al., 2012). These applications, however, did not consider the details of hydrological and erosion processes controlled by the conditions of karst development, and may have overestimated the erosion rates. Carbonate bedrocks (limestone or dolomite) forming slopes are characterized by high secondary porosity resulting in a well-developed underground drainage system. They often will outcrop directly at or near the surface, which facilitate the rapid transport of surface water to underground, even during a rainfall and runoff event (Williams, 1983). Runoff plot observations have demonstrated that the average runoff coefficient and sediment yield is very low on carbonate hillslopes under the humid climate (Imeson et al., 1998; Calvo-Cases et al., 2003; Chen et al., 2012a; Peng and Wang, 2012). Heterogeneous karst surfaces with various densities of the epikarst zone also generate

* Corresponding author at: Institute of Subtropical Agriculture, Chinese Academy of Sciences, Mapoling, Changsha, Hunan 410125, China.
E-mail address: hbchs@isa.ac.cn (H. Chen).

http://dx.doi.org/10.1016/j.geomorph.2015.10.013
0169-555X/

extremely complex runoff and erosion patterns. The discontinuous overland flow and sediment deposition patterns along karst hillslopes have been well documented (Calvo-Cases et al., 2003; Chang, 2011). Because of this discontinuity, the slope length factor (*L*) of the RUSLE in karst areas must be smaller than in non-karst areas with similar topography to effectively represent shorter flow lengths. Therefore, the *L* factor needs to be calibrated to accurately estimate soil erosion rates on karst hillslopes.

This study investigated two typical karst peak-cluster depression basins in southwestern China. Soil erosion monitoring has been insufficient in these areas. Attention is paid to the potential of using the ^{137}Cs tracer technique, which can provide retrospective soil redistribution information to evaluate the RUSLE model. The ^{137}Cs tracer technique has been widely used throughout the world (e.g., Owens and Walling, 1996; Navas et al., 2013). It is an artificial radionuclide with a half-life of 30.17 years, produced by nuclear bomb tests, and primarily deposited on the ground as fallout with precipitation from the 1950s to the early 1970s (Campbell, 1983). The use of ^{137}Cs as tracer is based on the assumption of its spatially uniform distribution across the landscape. It relies on the fact that ^{137}Cs binds immediately and strongly to fine particles in the topsoil, particularly clay minerals and humic materials, and is resistant to downward leaching and plant uptake. This results in redistribution of ^{137}Cs nearly exclusively in association with soil particles (Ritchie and Mchenry, 1990; Zapata, 2002). The use of this technique for soil erosion assessment may be generally grouped into two categories. First, the rates of net medium-term (40–50 years) soil loss or deposition are obtained by measuring spatial patterns of ^{137}Cs in both vertical and horizontal planes across the landscape (Walling and He, 1999). Second, sediment accumulation rates and yields from catchment can be calculated by measuring the ^{137}Cs inventory of sediment cores in various depositional systems such as lakes or reservoirs (He et al., 1996; Ritchie et al., 2009). In karst areas of southwestern China, previous studies (Li et al., 2009) on the characteristics of ^{137}Cs distribution indicated that the current ^{137}Cs conversion models may not be used for estimating soil redistribution rates at karst hillslopes because of the thin soil covering and the dissolution of carbonate grain in soils. However, there exists a unique landform type in southwestern China, the peak-cluster depression, which is a closed and flat depression surrounded by a series of hills. Depressions characterized by blocked or waterlogged conditions could be regarded as depositional systems. The mean soil erosion rates of the surrounding hillslopes and the deposition rates in the depressions counterbalance each other in a peak-cluster depression basin. A thick and uniform sediment layer in the depressions meets the basic requirement of ^{137}Cs method (Zapata, 2002). Some researchers have successfully estimated the sediment accumulation rates by measuring ^{137}Cs of sediment profiles in several cultivated depressions in southwestern China (Li et al., 2010; Bai, 2011).

The objectives of this research were to: (1) calibrate the RUSLE model on karst hillslopes mainly by adjusting the RUSLE-*L* factor based on the runoff plots data; (2) apply the calibrated RUSLE model to estimate the annual soil erosion rates on hillslopes and detect the sediment deposition characteristics by measuring ^{137}Cs in the depressions of the study basins; and (3) compare the RUSLE-simulated results with the ^{137}Cs records.

2. Materials and methods

2.1. Study area

This study was conducted at Huanjiang County (24°44′–25°33′N, 107°51′–108°43′E), northwest Guangxi in southwestern China (Fig. 1a). The area is underlain by limestone of the late Carboniferous age and mainly characterized by peak-cluster depression systems. The area has a warm subtropical monsoon climate where the rainy season coincides with higher temperatures. The mean annual temperature is 18.5 °C and the mean annual rainfall is about 1390 mm, almost 75% of which occurs from May to September (Chen et al., 2012a).

The runoff plots (Fig. 2a) were located in the lower part of a hillslope in Mulian Village (24°44′N, 108°18′E) and belong to the Huanjiang Observation and Research Station for Karst Ecosystems under the Chinese Academy of Sciences (CAS). The surface runoff and soil loss from these plots have been collected since 2006 using standard methods for RUSLE-type plots (Wischmeier and Smith, 1978). The three runoff plots under natural scrubland, grassland and cropland, respectively, were selected for calibration. They were all 20 m wide and had an area of 0.14, 0.21 and 0.19 ha respectively (Chen et al., 2012a). The slope of the plots varied from 4% to 97%.

The two peak-cluster depression basins (Fig. 2b, c) with different land uses are located near Guzhou Village (24°55′N, 107°56′E). One basin (referred to as GZ1) covers a drainage area of 31.1 ha with a depression area of 0.4 ha. Part of the GZ1 basin, including the entire depression and the lower part of all slopes, has been cultivated and subsequently serious land degradation and rock desertification has taken place. The rest of the GZ1 basin is covered by forests, shrubs and grassland. The grassland was relatively sparse and changed from cropland in 2004 at the northern hillslope in the GZ1 basin. The elevation ranges between 500 and 753 m a.s.l. and no outcropped sinkhole was found in the depression. The other

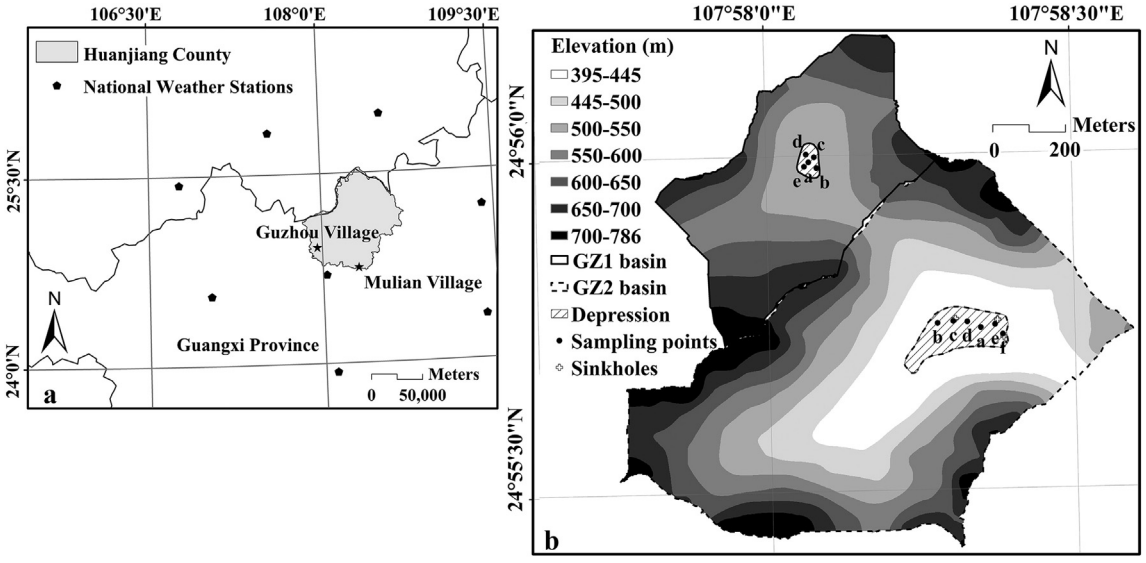

Fig. 1. Locations, the digital elevation model and ^{137}Cs sampling profiles of the study basins.

Fig. 2. Photos of the runoff plots (a) and the hillslopes of the GZ1 (b) and GZ2 (c) basins.

basin (referred to as GZ2) has not been used for agriculture but for light grazing and tree-cutting since the original forest was removed several hundred years ago. It has a drainage area of 80.4 ha with elevations ranging from 395 to 785 m a.s.l. The depression with an area of 2.7 ha is dominated by grass, while the surrounding slopes are mainly covered with secondary forestland and scrubland. In the entire GZ2 basin, the land use has not changed significantly since the 1950s. In addition, four sinkholes with the diameter all less than 1 m were located at points east, northeast and slightly north from the center of the depression (Fig. 1b). The sinkhole in the eastern part is near the toe of the slope and is enclosed by stones. The depression is waterlogged during the rainy season, with detention time of 2–3 days due to the high ground water levels and relatively poor drainage capacity of the underground porosities and pipelines.

2.2. Application and calibration of the RUSLE

The two study basins were discretized into uniform morphological units (i) and the following RUSLE model was applied to estimate the spatial distribution of the annual soil erosion rates on the surrounding hillslopes (EY_i; Mg ha^{-1} y^{-1}):

$$EY_i = R_i\, K_i\, L_i\, S_i\, C_i\, P_i \tag{1}$$

where R_i is the rainfall erosivity factor (MJ mm ha^{-1} h^{-1} y^{-1}), K_i is the soil erodibility factor (Mg ha^{-1} y^{-1} per unit R), L_i is the slope length factor (dimensionless), S_i is the slope steepness factor (dimensionless), C_i is the cover management factor (dimensionless), and P_i is the support practice factor (dimensionless).

R_i was computed as the sum of the storm erosivity index ($E \times I_{30}$) of the total number of erosive storm events for the whole year, where E is the energy of rainstorm (MJ ha^{-1} y^{-1}) and I_{30} (mm h^{-1}) is the maximum intensity in 30 minutes. E was estimated by rainfall intensity (I; mm h^{-1}) based on the following equation (Brown and Foster, 1987):

$$E = 0.29\left[1 - 0.72e^{(-0.05I)}\right]. \tag{2}$$

K_i was estimated based on the decimal logarithm of the geometric mean of the particle-size distribution (D_g), the logarithm of geometric standard deviation of D_g (S_g) and the soil organic matter (SOM) according to Borselli et al. (2012).

L_i and S_i were computed through an interaction between topography and flow accumulation (Moore and Bruch, 1986). The L-factor was generated from DEMs using LS-TOOL developed by Zhang et al. (2013), which was based on the following expressions of McCool et al. (1989). We chose to use high resolution 1-m DEMs as source data which were created based on 1:2000 topographic datasets.

$$L_i = (\lambda_i/22.13)^{m_i} \tag{3}$$

$$m_i = \beta_i/(1+\beta_i) \tag{4}$$

$$\beta_i = sin\theta/\left[3\cdot(sin\,\theta)^{0.8} + 0.56\right] \tag{5}$$

where λ_i is the length of the slope, m_i is a variable length-slope exponent, β_i is a factor that varies with slope gradient, andθ is the slope angle. LS-TOOL uses a unit contributing area algorithm to calculate λ_i of slope segment and allows cutoffs for the accumulated slope length at the location where deposition occurs or the cumulative area reaches the user specified threshold. The minimum set of the accumulated area threshold in LS-TOOL is equal to the area of one grid cell. The S-factor is evaluated based on McCool et al. (1987):

$$S_i = 10.8\sin\theta + 0.03 \quad (\text{slope length}>4.6\text{ m}, Si<9\%) \tag{6}$$

$$S_i = 16.8\sin\theta - 0.50 \quad (\text{slope length}>4.6\text{ m}, Si\geq 9\%) \tag{7}$$

$$S_i = 3.0(sin\,\theta)^{0.8} + 0.56 \quad (\text{slope length}<4.6\text{ m}). \tag{8}$$

C_i and P_i were obtained from published values for southwestern China (Xu et al., 2009). C_i was assigned values of 0.008, 0.01, 0.1 and 0.22 for forestland, scrubland, grassland and cropland, respectively. P_i was set to 0.5 for cropland and 1 for other land uses due to the absence of erosion control works.

If the area of the depression (A_d; ha), the area of the hillslopes (A_h; ha) and the sediment trap efficiency (STE; %) are known, the mean deposition rates of the depressions (DY_d; Mg ha^{-1} y^{-1}) can be determined from the average annual soil erosion rates of the surrounding hillslopes in the basins (EY_h; Mg ha^{-1} y^{-1}) as shown by (Li et al., 2010):

$$DY_d = EY_h \cdot A_h \cdot STE/A_d. \tag{9}$$

Precipitation and the annual sediment yield data for 2006 to 2010 from the three runoff plots were collected for calibration. There were 15 sets of data (5 years × 3 plots). The RUSLE-L factor was adjusted by reducing the accumulated area threshold to bring the model-estimated soil erosion rates within the range of the observed sediment yield. The minimum constraint of the accumulated area threshold in LS-TOOL is the area of the cell size of DEM datasets. For identifying the permissible coarsest resolution, the initial 1-m DEMs were thinned to generate a set of DEMs with grid size of 2, 3 and 5 m. The calibration started from setting the accumulated area threshold as the runoff plot area using DEMs with a grid size of 5 m. The model performance was evaluated using the root mean square error ($RMSE$) (Thomann, 1982) and model efficiency (ME) (Nash and Sutcliffe, 1970), defined as:

$$RMSE = \sqrt{\sum (O_j - P_j)^2/n} \tag{10}$$

$$ME = 1 - \sum (O_j - P_j)^2 / \sum (O_j - O_m)^2 \tag{11}$$

where O_j and P_j are the observed sediment yield and predicted output for the j-th pair, n is the total number of paired values, and O_m is the mean of n observed values. The smaller the *RMSE*, the closer the predicted values to the observed ones. The possible range for ME is $-\infty$ to 1, and the closer the value to 1, the better the predictions. A value less than zero indicates that the mean value of the output is a better estimate than the model prediction. Once calibrated, the RUSLE model was run for the two basins with the calibrated accumulated area threshold.

Due to the limitation of the rain gauge in Guzhou Village having no long-time continuous rainfall data, the precipitation information was all collected from the Mulian automated observation station of the Huanjiang Observation and Research Station for Karst Ecosystems under CAS. The Mulian station established in 2006 is located nearly 40 km away from Guzhou Village (Fig. 1a). The hourly rainfall values were used to characterize the precipitation of each rainfall event and the rainfall intensity during 2006–2011. Soil loss in karst areas of southwestern China is mostly caused by heavy storms with a rainfall depth of >40 mm and a maximum 30 minutes rainfall intensity > 30 mm h^{-1} (Peng and Wang, 2012). The average annual RUSLE-*R* value in the runoff plots and the study basins was calculated to be 2337.9 (MJ mm ha^{-1} h^{-1} y^{-1}) during the period 2006–2011. In order to verify the reliability of the precipitation data and conduct a better comparison with ^{137}Cs records for the two study basins, the annual rainfall data obtained from the eight national stations (Fig. 1a) were interpolated to characterize precipitation during 1963–2011. The mean annual precipitation (1446 mm) during 2006–2011 at the Mulian station was 0.5% higher than the average interpolating rainfall (1439 mm) of the two study basins during 2006–2011, while it was 3.6% lower than the average interpolating value (1499 mm) of the study basins during 1963–2011.

In each runoff plot, eight soil samples were collected at the depth of 0–20 cm for the soil texture and SOM analysis. The data of soil texture and SOM for different land uses were also obtained from the previous work in Guzhou Village (Chen et al., 2012b). The initial land use map of the study basins was made from September 2007 SPOT images with the resolution of 5 m using supervised classification methods controlled by a field survey. Six land uses were identified including cropland, grassland, forestland, scrubland, bare rock and land for traffic in the basin, based on the Chinese national standard of land use classification established by the Inspection and Quarantine of General Administration of Quality Supervision and Standardization Administration of China (2007). During each simulation, all the grid layers of the RUSLE factors were adjusted into the same cell size.

2.3. ^{137}Cs method

The basic principles of ^{137}Cs measurement were adopted from Zapata (2002) and Li et al. (2010). In a peak-cluster depression, it could be assumed that the only sources of ^{137}Cs in the depressions are direct atmospheric fallout and deposition of sediment-associated ^{137}Cs from the surrounding hillslopes. To determine the deposition rates in the depressions (*DY*; Mg ha^{-1} y^{-1}) from ^{137}Cs, the Simplified Mass-Balance Model and the Profile Shape Model were used for cultivated land and undisturbed land, respectively (Walling et al., 2002).

Soil sampling for ^{137}Cs measurement was conducted in the depressions of the two basins in September, 2011. Five sampling points were identified at the center and four corners of the GZ1 depression and six points at regular 40 m intervals along the central axis of the GZ2 depression (Fig. 1b). In each depression, one detailed sectioned profile was sampled by digging a pit and collecting soil samples at 2 cm depth interval from aside of the pit within an horizontal area of 10×15 cm^2. All the other profiles were sampled at 10 cm depth interval using a 5.2 cm diameter soil auger. In order to collect the entire ^{137}Cs inventory the sampling depth varied from 50 to 70 cm (down to the bedrock) in the GZ1 depression, and was 100 cm in the GZ2 depression. In addition, the area and topography of the depressions were measured using an electronic total station. The depth of the plow layer was measured manually when the local farmers plowed fields in the GZ1 basin. All the soil samples were air-dried, crushed, passed through a 2 mm mesh sieve to remove coarse material and sent to the Chengdu Institute of Mountain Hazards and Environment, CAS. The ^{137}Cs content of each sample was measured by γ spectrometry system consisting of a hyper pure coaxial germanium detector and a multichannel analyzer. The sample weights used for analysis were 250 g or more, and were counted for a minimum of 50,000 s and ^{137}Cs activity was determined from 662 keV peak on the spectrum. The results were reported with a precision of approximately $\pm$5% at the 95% probability level. They were originally calculated on a unit mass basis (Bq kg^{-1}) and were then converted to the total inventory (Bq m^{-2}) using the total weight of bulked core soil sample and the sampling area (Walling and Quine, 1990). Because it is difficult to find an ideal flat reference site in the study basins, the local ^{137}Cs inventory was referenced as 998 Bq m^{-2} measured in 2006 in Luoyang Town which was about 6 km away from the study area (Li et al., 2010). The reference inventory for 2011 was 888 Bq m^{-2} corrected for radioactive decay.

3. Results

3.1. RUSLE model

3.1.1. Model calibration

The results of regression and *ME* statistics between the simulated sediment yield by the RUSLE and the observed data with a series of the accumulated area threshold in the three runoff plots were shown in Table 1. The *RMSE* decreased significantly with the decrease of the accumulated area threshold, which indicated the effect of the slope or flow length on the accuracy of the RUSLE model and, therefore, the need to be calibrated on karst hillslopes. An accumulated area threshold of 1 m^2 (i.e. the grid cell size as 1 m) resulted in the best estimate of soil erosion rate as indicated by the smallest *RMSE* (0.097) and *ME* closest to one (0.84). As a result, the model was run with an accumulated area threshold of 1 m^2 using 1-m DEMs for both study basins. Nevertheless, the slope of the regression equation comparing measured annual sediment yields with the predicted ones was 0.82 indicating that RUSLE would overestimate the soil erosion rates by 18% even under the best setting (Table 1).

3.1.2. Model simulation

The maps of land use, the RUSLE-*K* factor and the slope inclination of the GZ1 and GZ2 basins are shown in Fig. 3. The value of K_i ranged from 0.015 (Mg ha^{-1} y^{-1} per unit R) for forestland above 550 m to 0.027 for cropland (Fig. 3b). Both basins are characterized by long and steep slopes. Slopes in excess of 25° (46%) cover respectively 76% and 85% of the two basins areas (Fig. 3c). The average length of hillslopes was 205 m in the GZ1 basin and 306 m in the GZ2 basin. The RUSLE-*L* and *S* factors are shown in Fig. 4. The estimated maximum values of flow

Table 1
Statistical analysis comparing the RUSLE-measured annual sediment yield (Mg ha^{-1} y^{-1}) with predictions for different accumulated area threshold in the runoff plots.

Accumulated area threshold (m^2)	Regression statistics			*ME*[a]	*RMSE*[b]
	Slope	*Int.*[c]	R^2		
Runoff plots area	0.019	−0.01	0.92	−3631	14.50
500	0.02	−0.01	0.92	−3168	13.55
200	0.05	−0.01	0.92	−417.4	4.922
25	0.26	−0.01	0.92	−10.2	0.806
9	0.51	−0.03	0.92	−0.58	0.303
4	0.69	−0.02	0.92	0.57	0.158
1	0.82	−0.02	0.92	0.84	0.097

[a] Model efficiency.
[b] The root mean square error.
[c] The intercept of linear equation.

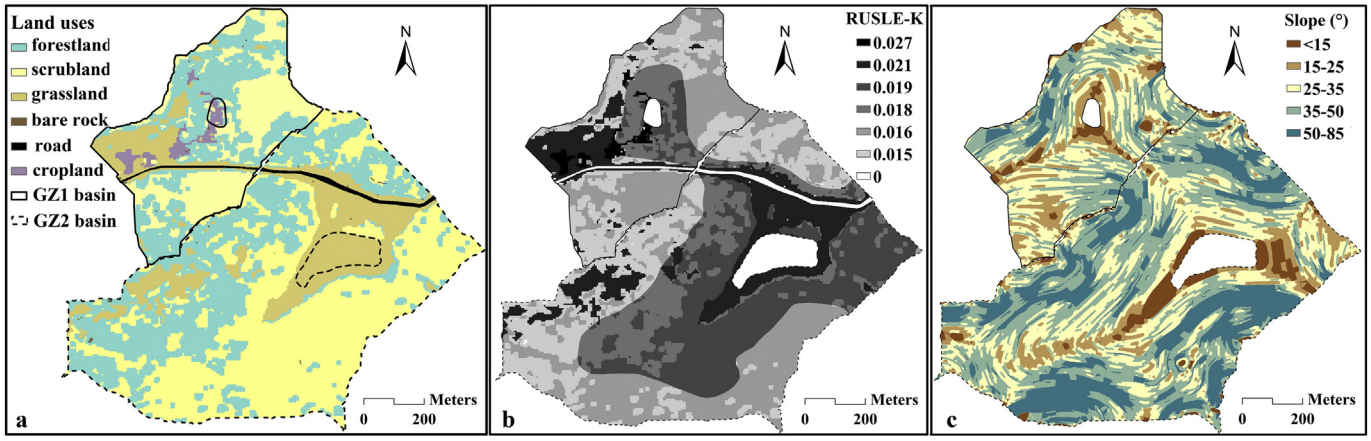

Fig. 3. Maps of land use, RUSLE-*K* factor and the slope inclination of the GZ1 and GZ2 basins.

length were much shorter than the length of hillslopes in both basins. The RUSLE-*L* factor (Fig. 4a) varied from 0.057 to 1.0 with an average of 0.086 in the GZ1 basin and from 0.057 to 0.99 with an average of 0.091 in the GZ2 basin. The highest *L* factor was found in flat areas. The RUSLE-*S* factor (Fig. 4b) had mean values of 2.1 and 2.6 in the GZ1 and GZ2 basins, respectively.

The results of the estimated annual soil erosion rates on hillslopes during the period of 2006 to 2011 are shown in Fig. 4c. The simulated soil erosion rates ranged from 0 to 3.85 Mg ha^{-1} y^{-1} with an average of 0.22 Mg ha^{-1} y^{-1} in the GZ1 basin, and from 0 to 0.70 Mg ha^{-1} y^{-1} with an average of 0.10 Mg ha^{-1} y^{-1} in the GZ2 basin. The depression in the GZ1 basin has no sinkholes; therefore, all of the sediments from hillslopes are trapped in the depression ($STE = 1$). In the GZ2 basin, considering that most of soil loss is caused by heavy rainfall storms during which the depression was usually waterlogged with a detention time reaching 2–3 days, 80% of the sediment eroded from hillslopes was estimated to be trapped in the depression ($STE = 0.8$; Li et al., 2010; Bai, 2011). Average annual deposition rates estimated using Eq. (2) were 14.40 and 2.29 Mg ha^{-1} y^{-1} in the depressions of the GZ1 and GZ2 basins, respectively.

The erosion risk categories for each land use type estimated by RUSLE were classified (Table 2), including low (<0.3 Mg ha^{-1} y^{-1}), medium (0.3–1 Mg ha^{-1} y^{-1}) and severe (>1 Mg ha^{-1} y^{-1}). In the GZ1 basin, the annual soil erosion rates were low for 81% of the hillslopes, covering all the forestland and scrubland. Medium erosion was found on 13% of the area (79% of grassland and 47% of cropland). The remaining 5% of the hillslopes under grassland and cropland was estimated to be suffered from severe erosion. In the GZ2 basin, 98% of hillslopes were estimated to have low erosion rates, including all the forestland, scrubland and 93% of the grassland. Only 1% of the area was simulated to have medium erosion rates.

3.2. ^{137}Cs records

The vertical distribution and the total inventory of ^{137}Cs in the five sediment profiles at the depression of the GZ1 basin is shown in Fig. 5. The detailed sectioned profile (Fig. 5a) shows that ^{137}Cs concentration tended to be evenly distributed within 0.28 m. ^{137}Cs concentration was the highest at 0.18–0.20 m depth (6.1 Bq kg^{-1}), and decreased slightly to 2.8 Bq kg^{-1} at 0.26–0.28 m depth. The plow layer depth was measured to be 0.18 m in the depression. The ^{137}Cs distribution depth was greater than the plow depth which showed a progressive accretion of soil at the surface. A very small amount of ^{137}Cs below 0.28 m might have resulted from the downward diffusion and migration process. In the other four sampling cores, ^{137}Cs activity was primarily detected in the upper three sampling layers (0–0.30 m). The ^{137}Cs inventories ranged from 1125 to 1904 Bq m^{-2}, with a coefficient of variation (*CV*) of 20.9%. They were all in excess of the local reference inventory (888 Bq m^{-2}), which indicated the presence of sediment deposition in every profile. Less deposition was observed at the four corners of the depression in the GZ1 basin. Using the simplified mass–balance model, the annual deposition rates of the five sediment profiles were calculated to be 6.81 to 29.35 Mg ha^{-1} y^{-1} with a mean of 15.80 Mg ha^{-1} y^{-1} during the period 1963–2011.

The ^{137}Cs profiles and corresponding total inventory for the six sampling points in the depression of the GZ2 basin are shown in Fig. 6. The

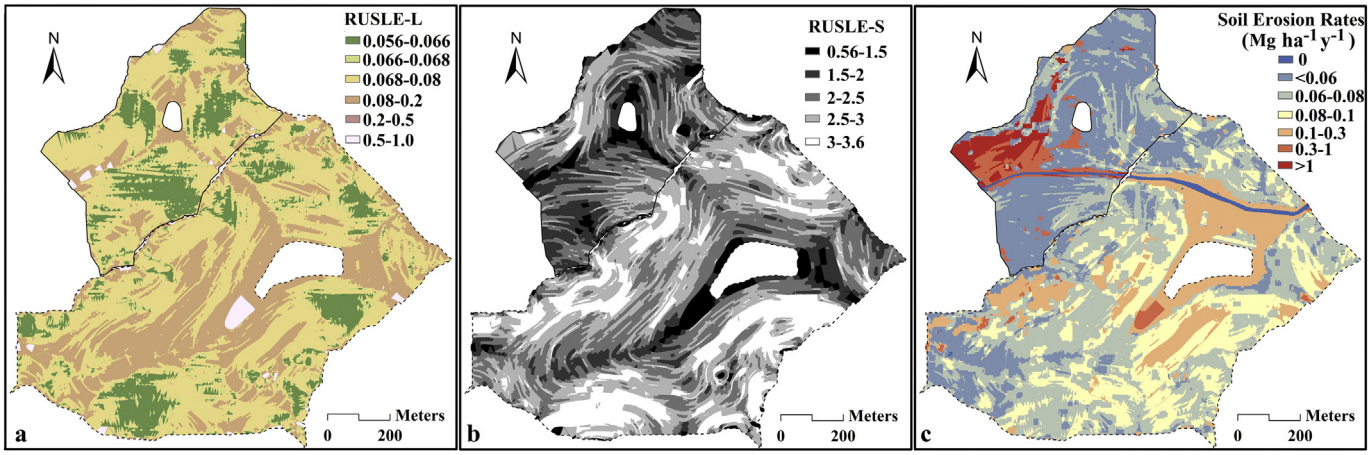

Fig. 4. Maps of RUSLE-*L*, *S* factor and the RUSLE-estimated annual soil erosion rates during 2006–2011 in the GZ1 and GZ2 basins.

Table 2
Area for each erosion category and the average soil erosion rates estimated by the RUSLE model for different land uses in the GZ1 and GZ2 basins.

Land uses		Area (ha) for each erosion categories (Mg ha^{-1} y^{-1})					Average erosion rate (Mg ha^{-1} y^{-1})
		No erosion	<0.3	0.3–1	>1	Total	
GZ1 basin	Forestland	–	12.7	–	–	12.7	0.05
	Scrubland	–	12.0	–	–	12.0	0.06
	Grassland	–	–	3.4	0.9	4.3	0.91
	Cropland	–	–	0.6	0.7	1.3	1.15
	Others [a]	0.4	–	–	–	0.4	–
	Total	0.4	24.7	4.0	1.6	30.7	0.22
GZ2 basin	Forestland	–	27.2	–	–	27.2	0.06
	Scrubland	–	38.7	–	–	38.7	0.09
	Grassland	–	10.2	0.8	–	11.0	0.26
	Others[a]	0.8		–	–	0.8	–
	Total	0.8	76.1	0.8	–	77.7	0.10

[a] Road and bare rock.

^{137}Cs concentration peak is located at the surface layer of 0–0.02 m in the detailed sectioned profile (Fig. 6a). It declined exponentially with increase in depth and dropped below 1 Bq kg^{-1} near 0.20 m. The depth distribution shape of ^{137}Cs in all the other five profiles was similar to the profile in Fig. 6a, confirming that the site has not been cultivated since the initial isotope fallout. The ^{137}Cs inventories varied from 754 to 1743 Bq m^{-2}, with a *CV* value of 34.1%. Greater deposition was observed at profiles c and e, which were located near two groups of sinkholes. Except for profile d, the ^{137}Cs inventory of all profiles was in excess of the local reference inventory (888 Bq m^{-2}). This indicates that soil deposition occurred in profiles a, b, c, e and f, and soil erosion might have occurred in profile d. According to the profile shape model (Walling et al., 2002), the annual deposition rates of the six sampling profiles varied from −1.40 to 8.48 Mg ha^{-1} y^{-1} with the mean value of 2.84 Mg ha^{-1} y^{-1} during the period 1963–2011.

4. Discussion

The depressions in the GZ1 and GZ2 basins are relatively small covering 1.5% and 3.4% of their respective watershed areas. They are well defined and characterized by flat relief with elevation differences not exceeding 2 m. The *CV* value of ^{137}Cs inventories was 20.9% and 34.1% for the depressions in the GZ1 and GZ2 basins, respectively. These values agree well with *CV* values commonly reported in the literature for homogeneous sites (Owens and Walling, 1996; Sutherland, 1996). ^{137}Cs is a moderately variable (*CV* = 15–35%) soil property (Sutherland, 1996) where random spatial variability is the most influential factor affecting the overall uncertainty of its measurement (Owens and Walling, 1996). Due to the nature of the accumulation processes on the sites (closed depression with frequent prolonged waterlogging) the observed *CV* might be associated with the sampling position. Indeed, greater deposition (and greater ^{137}Cs inventory) occurred in the middle of the depression, near sinkholes, while lesser deposition was found near its edges. Similar observations were made by Li et al. (2010) and Bai (2011) who studied karst landscapes in the same region.

The simulated results by the calibrated RUSLE model showed that the mean annual deposition rates in the depressions were 14.40 Mg ha^{-1} y^{-1} in the partially cultivated (GZ1) basin and 2.29 Mg ha^{-1} y^{-1} in the undisturbed (GZ2) basin during 2006–2011. They were slightly lower than the mean deposition rates quantified by ^{137}Cs profiles, which was 15.80 and 2.84 Mg ha^{-1} y^{-1} in the depressions of the GZ1 and GZ2 basins, respectively, during 1963–2011. The annual precipitation during 2006–2011 was 3.6% lower than that during 1963–2011. The land use has not changed significantly since the 1950s except for the northern hillslope in the GZ1 basin, which was converted from cropland to grassland in 2004. Hence, the annual deposition rates in the depressions predicted by RUSLE should be slightly lower than those measured by the ^{137}Cs technique. The average annual soil erosion rates of hillslopes simulated by RUSLE were 0.22 and 0.10 Mg ha^{-1} y^{-1} in the GZ1 and GZ2 basins during 2006–2011. Several researchers observed erosion processes on runoff plots in other karst areas. Kosmas et al. (1997) reported the erosion rates of 0–1.42 Mg ha^{-1} y^{-1} on limestone landscape under different land uses in the Mediterranean region. Peng and Wang (2012) reported the annual soil loss of less than 0.69 Mg ha^{-1} y^{-1} between 2008 and 2010 in Guizhou Province of southwestern China. These results were all in good agreement with our study. However, the estimated annual soil erosion rates were smaller than those reported for other non-karst areas with similar latitudes. For example, in the hilly Sichuan basin and the Three Gorges area in southern China, the annual soil loss rates of purple soil measured by the ^{137}Cs technique were 7.6–98.5 Mg ha^{-1} y^{-1} on cultivated slopes with gradients of 9%–60%, and 3.1–6.9 Mg ha^{-1} y^{-1} on uncultivated slopes (Feng et al., 2004; Shi et al., 2012). The main reason of such differences is that the thin soil layer and the well-developed epikarst zone of carbonate bedrock play a very important role in runoff and erosion processes on karst hillslopes (Williams, 1983; Peng and Wang, 2012). Due to the high permeability and storage capacity of the epikarst zone under the humid climate, most rainfall water was transported underground

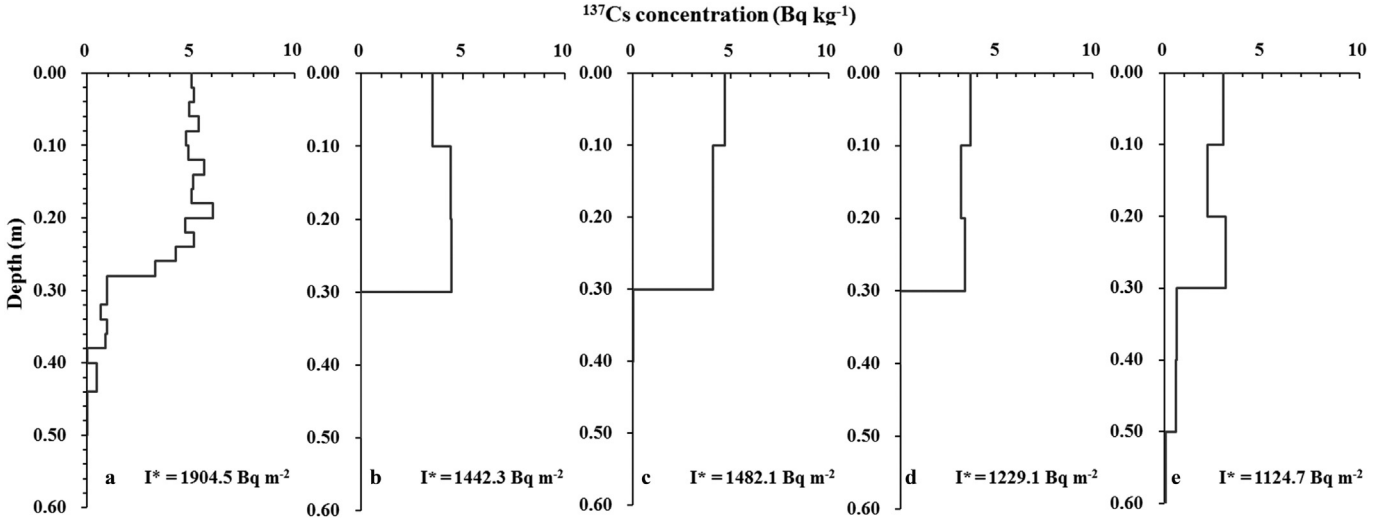

Fig. 5. Vertical distribution of ^{137}Cs in sediment profiles at the depression of the GZ1 basin.

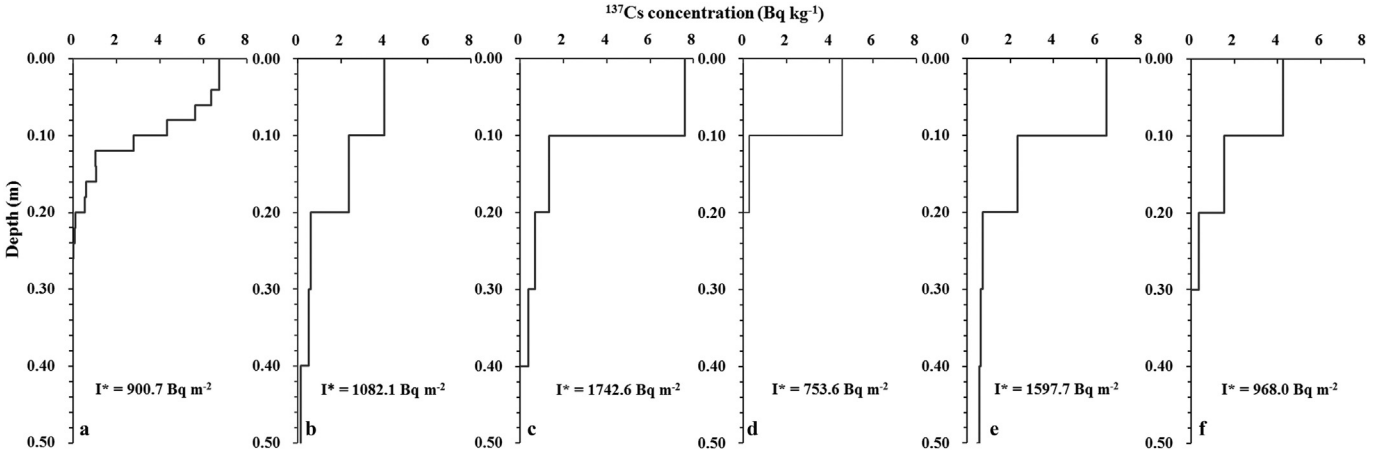

Fig. 6. Vertical distribution of ^{137}Cs in sediment profiles at the depression of the GZ2 basin.

and the runoff coefficient on karst hillslopes was negligible, generally less than 10% (Calvo-Cases et al., 2003; Chen et al., 2012a; Peng and Wang, 2012). The heterogeneous development and distribution of the epikarst zone determines that the karst hillslopes behave as a fragmented patchwork of runoff and run-on areas (Chang, 2011). As shown in our study, the accumulated area threshold of the overland flow on karst hillslopes can be small (1 m), whereas in non-karst areas this value may reach as much as 120 m (Fu et al., 2006). Therefore, the proposed RUSLE methodology could be effective in estimating the soil erosion rates on karst hillslopes, if particular attention is given to the accumulated area threshold and calibration of the slope length factor. High resolution DEM datasets may be required. Moreover, there is still much room to improve the spatial accuracy of the RUSLE-*K* and *C* factors in this study.

Soil formation rate in karst areas of southwestern China has been estimated between 0.04 and 1.2 Mg ha^{-1} y^{-1} (Li et al., 2006; Cao et al., 2008). According to our measurements, the mean annual soil erosion rates of each land use ranged from 0.05 to 1.15 Mg ha^{-1} y^{-1} during 2006–2011. Soil layers on hillslopes especially for cropland could be diminishing gradually. Moreover, soil creeping to the underground through dissolution channels also has been observed on karst hillslopes (Zhang et al., 2011). Therefore, the erosion hazard of the study basins is still quite high and should not be ignored. Natural vegetation protection with engineering measures on cropland was suggested to be the first important approach to maintain the surface soil on karst hillslopes in the study region.

5. Conclusion

The peak-cluster depression basins in a karst area of southwestern China provided an opportunity to study soil erosion on the surrounding karst hillslopes and compare it with the deposition records in the central depressions. The application of the calibrated RUSLE model allows detailed mapping of spatially distributed soil erosion rates on hillslopes in the two peak-cluster depression basins (GZ1 and GZ2). The accuracy of the RUSLE model was greatly affected by the slope or flow length because of the discontinuous nature of the overland flow due to rapid and significant underground seepage on karst hillslopes. The slope length factor (*L*) in the study basins is best estimated by setting the accumulated area threshold as 1 m^2 using a 1-m DEM. The predicted mean soil erosion rates on hillslopes using the calibrated RUSLE model agreed well with ^{137}Cs measurements in the depressions. Calibration of RUSLE-*L* factor is necessary for an effective application of the RUSLE model on karst hillslopes.

In the GZ1 and GZ2 basins, the average values of the *L* factor were estimated to be 0.086 and 0.091, respectively, where the average hillslope length was 205 and 306 m. The RUSLE estimated average annual soil erosion rate on the surrounding hillslopes was 0.22 Mg ha^{-1} y^{-1} in the partially cultivated GZ1 basin and 0.10 Mg ha^{-1} y^{-1} in the undisturbed GZ2 basin during 2006–2011. The mean annual soil erosion rates for each land use in the two basins ranged from 0.05 to 1.15 Mg ha^{-1} y^{-1}. The erosion hazard especially for cropland is high and should not be ignored due to the shallow soil layer and the low soil formation rates in the studied karst basins.

Acknowledgments

This research was funded by grants from the National Key Basic Research Program of China (2015CB452703), the Action Plan for the Development of Western China of Chinese Academy of Sciences (KZCX2-XB3-10), and the National Natural Science Foundation of China (51379205). We would like to thank Tonggang Fu, Jing Yang, Chuan Zhang and Ke Hu (Institute of Subtropical Agriculture, CAS) for their kind assistance in field sampling. We also would like to thank Dr. Mark Nearing (USDA-ARS, Tucson, AZ), the reviewers and the editor for their helpful suggestions to improve this paper.

References

Bai, X., 2011. Assessment of sediment and erosion rates by using the caesium-137 technique in a Chinese polygonal karst depression. Environmental Earth Sciences 64, 2151–2158. http://dx.doi.org/10.1007/s12665-011-1042-8.

Borselli, L., Torri, D., Poesen, J., Laquinta, P., 2012. A robust algorithm for estimating soil erodibility in different climates. Catena 97, 85–94. http://dx.doi.org/10.1016/j.catena.2012.05.012.

Brown, L.C., Foster, G.R., 1987. Storm erosivity using idealized intensity distributions. Trans. Am. Soc. Agric. Eng. 30, 379–386.

Campbell, B.L., 1983. Applications of environmental caesium-137 for the determination of sedimentation rates in reservoirs and lakes and related catchment studies in developing countries. Radioisotopes in Sediment Studies Technology Document 7-30.

Cao, J.H., Jiang, Z.C., Yang, D.S., Pei, J.G., Yang, H., Luo, W.Q., 2008. Grading of soil erosion intensity in southwest karst area of China. Science of Soil and Water Conservation 6, 1–7 in Chinese.

Calvo-Cases, A., Boix-Fayos, C., Imeson, A.C., 2003. Runoff generation, sediment movement and soil water behavior on calcareous (limestone) slopes of some Mediterranean environments in southeast Spain. Geomorphology 50, 269–291. http://dx.doi.org/10.1016/S0169-555X(02)00218-0.

Chang, Y., 2011. The Mechanism of Overland Flow Yield in Peak-cluster Depression of Southern China. China University of Geosciences, Wuhan in Chinese.

Chen, H.S., Yang, J., Fu, W., He, F., Wang, K.L., 2012a. Characteristics of slope runoff and sediment yield on karst hill-slope with different land-use types in northwest Guangxi. Transactions of the Chinese Society of Agricultural Engineering 28, 121–126 in Chinese.

Chen, J., Chen, H.S., Feng, T., Wang, K.L., Zhang, W., 2012b. Anti-soil erodibility of different land use types in northwest Guangxi karst regions. Chinese Journal of Eco-Agriculture 20, 105–110 in Chinese.

Febles-Gonzalez, J.M., Vega-Carreno, M.B., Tolon-Becerra, A., Lastra-Bravo, X., 2012. Assessment of soil erosion in karst regions of Havana, Cuba. Land Degrad. Dev. 23, 465–474. http://dx.doi.org/10.1002/ldr.1089.

Feng, M.Y., Zhang, X.B., Wen, A.B., He, X.B., 2004. Assessment of soil loss on uncultivated slope land by using ^{137}Cs technique in the upper Yangtze River basin of China. International Journal of Sediment Research 19, 60–65.

Fu, G.B., Chen, S.L., Mccool, D.K., 2006. Modeling the impacts of no-till practice on soil erosion and sediment yield with RUSLE, SEDD, and ArcView GIS. Soil Tillage Res. 85, 38–49. http://dx.doi.org/10.1016/j.still.2004.11.009.

He, Q., Walling, D.E., Owens, P.N., 1996. Interpreting the ^{137}Cs profiles observed in several small lakes and reservoirs in southern England. Chem. Geol. 129, 115–131. http://dx.doi.org/10.1016/0009-2541(95)00149-2.

Inspection and Quarantine of General Administration of Quality Supervision, Standardization Administration of the China, 2007y. Current Landuse Condition Classification GB/T 21010-2007. Standards Press of China, Beijing in Chinese.

Imeson, A.C., Lavee, H., Calvo, A., Cerda, A., 1998. The erosional response of calcareous soil along a climatological gradient in Southeast Spain. Geomorphology 24, 3–16. http://dx.doi.org/10.1016/S0169-555X(97)00097-4.

Kosmas, C., Danalatos, N.G., Cammeraat, L.H., Chabart, M., Diamantopoulos, J., Farand, R., Gutierrez, L., Jacob, A., Marques, H., Martinez-Fernandez, J., 1997. The effect of land use on runoff and soil erosion rates under Mediterranean conditions. Catena 29, 45–59. http://dx.doi.org/10.1016/S0341-8162(96)00062-8.

Li, H., Zhang, X.B., Wang, K.L., Wen, A.B., 2009. ^{137}Cs distribution characteristics at a Talus-type karst slope in Northwestern Guangxi. J. Soil Water Conserv. 23, 42–47 in Chinese.

Li, H., Zhang, X.B., Wang, K.L., Wen, A.B., 2010. Assessment of sediment deposition rates in a karst depression of a small catchment in Huanjiang, Guangxi, southwest China, using the cesium-137 technique. Journal of Soil and Water Conservation 65, 223–232. DOI:doi:http://dx.doi.org/10.2489/jswc.65.4.223.

Li, Y.B., Wang, S.J., Wei, C.F., Long, J., 2006. The spatial distribution of soil loss tolerance in carbonate area in Guizhou province. Earth and Environment 34, 36–40 in Chinese.

McCool, D.K., Brown, G.R., Foster, G.R., Mutchler, C.K., Meyer, L.D., 1987. Revised slope steepness factor for the universal soil loss equation. Trans. Am. Soc. Agric. Eng. 30, 1387–1396.

McCool, D.K., Foster, G.R., Mutchler, C.K., Meyer, L.D., 1989. Revised slope length factor for the universal soil loss equation. Trans. Am. Soc. Agric. Eng. 32, 1571–1576.

Moore, I.D., Burch, G.J., 1986. Physical basis of the length-slope factor in the universal soil loss equation. Soil Sci. Soc. Am. J. 50, 1294–1298.

Nash, J.E., Sutcliffe, J.V., 1970. River flow forecasting through conceptual models part I — a discussion of principles. Journal of Hydrology 10, 282–290. http://dx.doi.org/10.1016/0022-1694(70)90255-6.

Navas, A., López-Vicente, M., Gaspar, L., Machín, J., 2013. Assessing soil redistribution in a complex karst catchment using fallout ^{137}Cs and GIS. Geomorphology 196, 231–241. http://dx.doi.org/10.1016/j.geomorph.2012.03.018.

Owens, P.N., Walling, D.E., 1996. Spatial variability of caesium-137 inventories at reference sites: an example from two contrasting sites in England and Zimbabwe. Appl. Radiat. Isot. 47, 699–707. http://dx.doi.org/10.1016/0969-8043(96)00015-2.

Parise, M., De Waele, J., Gutiérrez, F., 2009. Current perspective on the environmental impacts and hazards in karst. Environ. Geol. 58, 235–237. http://dx.doi.org/10.1007/s00254-008-1608-2.

Peng, T., Wang, S.J., 2012. Effects of land use, land cover and rainfall regimes on the surface runoff and soil loss on karst slopes in southwest China. Catena 90, 53–62. http://dx.doi.org/10.1016/j.catena.2011.11.001.

Renard, K.G., Foster, G.R., Weesies, G.A., Porter, J.P., 1991. RUSLE—revised universal soil loss equation. J. Soil Water Conserv. 46, 30–33.

Ritchie, J.C., Mchenry, J.R., 1990. Application of radioactive fallout cesium-137 for measuring soil erosion and sediment accumulation rates and patterns: a review. J. Environ. Qual. 19, 215–233. http://dx.doi.org/10.2134/jeq1990.00472425001900020006×.

Ritchie, J.C., Nearing, M.A., Rhoton, F.E., 2009. Sediment budgets and source determinations using fallout Cesium-137 in a semiarid rangeland watershed, Arizona, USA. J. Environ. Radioact. 100, 637–643. http://dx.doi.org/10.1016/j.jenvrad.2009.05.008.

Shi, Z.L., Wen, A.B., Zhang, X.B., He, X.B., Li, H., Yan, D.C., 2012. ^{137}Cs and ^{210}Pb as soil erosion tracers in the Hilly Sichuan Basin and the Three Gorges Area of China. J. Mt. Sci. 9, 27–33. http://dx.doi.org/10.1007/s11629-012-2200-5.

Sutherland, R.A., 1996. Caesium-137 soil sampling and inventory variability in reference locations: a literature survey. Hydrol. Process. 10, 43–53. http://dx.doi.org/10.1002/(SICI)1099-1085(199601)10:1<43::AID-HYP298>3.0.CO;2-X.

Thomann, R.V., 1982. Verification of water quality models. Journal of Environmental Engineering Division 108, 923–940.

Walling, D.E., Quine, T.A., 1990. Calibration of caesium-137 measurements to provide quantitative erosion rate data. Land Degrad. Dev. 2, 161–175. http://dx.doi.org/10.1002/ldr.3400020302.

Walling, D.E., He, Q., 1999. Improved models for estimating soil erosion rates from cesium-137 measurements. J. Environ. Qual. 28, 611–622. http://dx.doi.org/10.2134/jeq1999.00472425002800020027×.

Walling, D.E., He, Q., Appleby, P.G., 2002. Conversion models for use in soil-erosion, soil-redistribution and sedimentation investigations. In: Zapata, F. (Ed.), Handbook for the Assessment of Soil Erosion and Sedimentation Using Environmental Radionuclides. Kluwer Academic Publ, London, pp. 111–164.

Wang, S.J., Liu, Q.M., Zhang, D.F., 2004. Karst rocky desertification in southwestern China: geomorphology, landuse, impact and rehabilitation. Land Degrad. Dev. 15, 115–121. http://dx.doi.org/10.1002/ldr.592.

Williams, P.W., 1983. The role of the subcutaneous zone in karst hydrology. J. Hydrol. 61, 45–67. http://dx.doi.org/10.1016/0022-1694(83)90234-2.

Wischmeier, W.H., Smith, D.D., 1978. Predicting rainfall erosion losses: a guide to conservation planning. USDA Agric. Handbook 537. U.S. Gov. Print. Office, Washington, DC.

Xu, Y.Q., Peng, J., Shao, X.M., 2009. Assessment of soil erosion using RUSLE and GIS: a case study of the Maotiao River watershed, Guizhou Province, China. Environ. Geol. 56, 1643–1652. http://dx.doi.org/10.1007/s00254-008-1261-9.

Zapata, F. (Ed.), 2002. Handbook for the Assessment of Soil Erosion and Sedimentation Using Environmental Radionuclides. Kluwer Academic Publishers, London.

Zhang, H., Yang, Q., Li, R., Liu, Q., Moore, D., He, P., Ritsema, C.J., Geissen, V., 2013. Extension of a GIS procedure for calculating the RUSLE equation LS factor. Comput. Geosci. 52, 177–188. http://dx.doi.org/10.1016/j.cageo.2012.09.027.

Zhang, X.B., Bai, X.Y., He, X.B., 2011. Soil creeping in the weathering crust of carbonate rocks and underground soil losses in the karst mountain areas of southwest China. Carbonates Evaporites 26, 149–153. http://dx.doi.org/10.1007/s13146-011-0043-8.